6th Pacific RIM International Conference on Water Jet Technology, 9-11 October 2000, pp 88-94

ON A NEW DYNAMIC MATERIAL REMOVAL MECHANISM FOR ABRASIVE WATERJET MACHINING (AWJM)

ASHRAF I. HASSAN
and
JAN. KOSMOL

Department of Machine Technology, Technical University of Silesia, Konarskiego St., 18a, 44-100 Gliwice, Poland

Abstract: Modeling of abrasive waterjet machining (AWJM) has been finding widespread interest for the past twenty years. Due to the complex interaction of several AWJM parameters, combined with the nonlinear dynamic high speed impact of several thousands of small abrasive particles on the workpiece surface, the mechanism of material removal has not yet been fully understood. The current paper presents an attempt to explain the mechanism of material removal in AWJ, as a result of abrasive particle impact through step by step tracing of the abrasive particle as it is interacting with the workpiece material. The new model considers the elastic-plastic behavior of the workpiece material. Also the non linear dynamic loading conditions which are characteristic feautres of AWJM are accounted for in the pesent study. The failure of the workpiece material is examined analytically, by means of a virtual finite element (FE) AWJ experiment, and experimentally, by means of scanning electron microscopy (SEM) and surface topographies. Stress results indicate that the workpiece material is subject to severe highly localized plastic deformation and as a result, small overlapping craters are generated. These craters are formed by high compressive stresses at the cutting interface. The finite element results indicate a good agreement with experimental results.

1. Introduction

Abrasive waterjet machining (AWJM) has been finding widespread interest over the past few years. Due to the complex interaction of several parameters, including hydraulic, mechanical and abrasive material behavior, the mechanism of material removal, in this high-speed mechanical erosive process, has not yet been fully understood. ‘‘It was recognized that an impact between two solid bodies generates two different although interconnected events; phenomena at or in the immediate vicinity of the contact position and the propagation of a signal to distant points of the two bodies. For speeds less than 0.1 m/s, no significant waves will be produced, and hence the process can be regarded as occurring under quasi-static conditions. This impact is characterized by completely elastic behavior and the energy loss is a small portion of the total mechanical energy and can be neglected. On the other hand, for projectiles with hypervelocities, the lower bound of which is 3000 m/s, the generated stresses will exceed Young’s modulus.[1]’’. In explosive manufacturing processes such as explosive welding, ‘‘workpiece materials which are impacted at velocities exceeding 400 m/s, suffer from high stresses which may exceed 40,000 MPa. This phenomenon was explained by highly excited energetic states. Such energy significantly exceeds the internal energy of the workpiece materials, causing its destruction.[2]’’. Explosive or shock compaction technique is a potential method to consolidate hard to center powders. ‘‘In this technique, extremely high impact stresses, up to 25,000 MPa, are applied to the powder in a very short time, e.g. within several microseconds.[3]’’. One of the few linear dynamic FE studies of WJ was carried out by Alder[4]. Due to the linear analysis assumed, maximum compressive stress obtained was 480 MPa, when using a 2 mm diameter water drop traveling at a speed of 305 m/s. This level of low compressive stresses explains the inability of WJ to erode metals. Geskin et al. pointed out that, ‘‘erosion is characterized by multiple dimples resulting from particles’ impact. It was assumed that the distribution of the dimples was a measure of the distribution of the active particles having sufficient energy to deform the workpiece material. The structure of the surface results from overlapping of each individual crater.[5]’’. ‘‘The roughness of the surface is caused by the sum of individual micro removals by abrasive particles. Each crater and its overlapping with another leads to a random structure.[6]’’. Hashish found that ‘‘the surface roughness is related to the dynamics of the cutting process. The particle size is a significant factor in surface finish.[7]’’. A new approach of nonlinear dynamic modeling of AWJ using virtual FEM has been recently developed by the authors. ‘‘This approach consists of tracing the abrasive particle, from its early exit from the mixing tube nozzle to its reflection from the surface after interaction with the material at minute time intervals, e.g. 0.01 μs. Using this method, the depth of AWJ kerf and the developed flow stresses are now obtainable.[8]".

The objective of this paper is to explain the mechanism of material removal in AWJ as a result of abrasive particle impact in the deformation wear zone. This will be done through step by step tracing of the abrasive particle as it is interacting with the workpiece material. The new model considers the elastic-plastic behavior of the workpiece material. The extremely small time increments used here are helpful in precisely recording the high speed impact moment. Flow stresses generated as a result of impact could also provide deeper insight in explaining the high strain rate dynamic plastic deformation.

2. Experimental Work

A two dimensional abrasive waterjet machine, Foracon ORCA 2000, is used in the experimental work. The machine has the following specifications: work table dimensions of 2000 mm in the X axis, 3000 mm in the Y axis and 220 in the Z axis, accuracy of 0.15 mm, with maximum traverse rate (u) of 12 m/min. The high pressure intensifier pump used is model no. 9XVS-55, from Flow International Corp., with maximum pressure (P) of 380 MPa. The abrasive feed system enables abrasive flow rate (m_a) in the range of 0.25-10 g/s. A nozzle diameter (d_n) of 0.3 mm and mixing tube diameter (d_m) of 0.9 mm were used. Low carbon steel St3S, corresponding to Polish Standards PN-88/H-84020, was chosen as the workpiece material for AWJ experiments. Each sample has the following dimensions: 100*20*70 mm. The mechanical properties of the workpiece material are as follows: yield strength: 267 MPa, ultimate tensile strength: 409 MPa, Percentage elongation: 35, Young's modulus: 207 E3 MPa, Poisson's ratio: 0.3. Each specimen was cut to the abovementioned dimensions and the surface was machined and then ground on a surface grinding machine. The surface roughness (R_a) of each individual specimen, before AWJ machining, is in the range of 0.15-0.2 μm. Australian Paser garnet (GMA) from Flow Corp. with Mesh No: 80, was chosen as the abrasive material for experiments. The measuring machine used throughout this work for recording the workpiece 3D topographies and measuring kerf depth is Form Measuring Machine PG-2/200 M, and it has the following specifications: measurement range: ± 5 mm, speed of measuring head: 0.1, 0.2, 0.5, 1 mm/s, maximum measuring length: 200 mm, stylus radius: 20 μm, mapping stylus steel NW1 angle 11°, radius 25 μm. For photomicrographs, Jeol JXA-50A scanning electron microscope is used. Samples, with maximum dimensions of: Φ 8*10 mm, are cut from the machined samples both across and along the AWJ kerf using wire electro-discharge machine tool.

3. Theoretical Analysis

The process has been simulated using the finite element method (FEM). In order to get more accurate results, the time step is chosen as 0.01 μs. Due to symmetry of geometry, only one quarter of both the abrasive and workpiece model needs to be analyzed, which greatly reduces the computational requirements. The workpiece is divided into 20 nodded higher order nonlinear solid elements. A total number of 250 elements was used to model the workpiece with size of each element of 0.1 mm * 0.1 mm * 0.1 mm. The number of nodal points is 1566. The overall workpiece dimensions are 0.5 mm * 1 mm * 0.5 mm. The constitutive model used for the workpiece is chosen as Von Mises elastoplastic isotropic hardening with linear strain hardening. The abrasive particle is modeled using 16 twenty nodded solid elements. Linear elastic model is chosen for the abrasive particle material. The dimensions of each element are 0.1 mm*0.1 mm* 0.1 mm. The boundary conditions include a fixed support of the workpiece from the bottom as it is fixed on the table of the AWJ machine. The abrasive particle is allowed to move freely downwards perpendicular to the workpiece surface. Nine 3D Contact elements are added between the abrasive particle and the workpiece. They allow for complete interaction including transfer of momentum between the abrasive particle and the workpiece. The model was then analyzed on a Pentium II PC workstation and deformations and stresses in the workpiece material were obtained using ALGOR Accupak/VE nonlinear dynamic stress analysis and event simulation, Version 12 WIN. A detailed description of the FE model is found elsewhere.[8].

4. Results and Discussion

4.1 *Surface topographies*

Topographies of AWJ machined surfaces are shown in Fig. 1 below for two different pressures. The effect of abrasive particle impingement on the workpiece surface is clearly seen in the figure. The workpiece material plastically flows under the effect of the generated high speed pressure waves in two directions. The first one is the main direction of deformation; downwards at the center of the impact site, under the action of impact. The second one upwards, at the peripheral edges of the recently formed cavity to form burrs. As a result, a central crater is developed at the center of the impact site, surrounded by raised material. This mechanism of crater formation is the same at any value of pressure used.

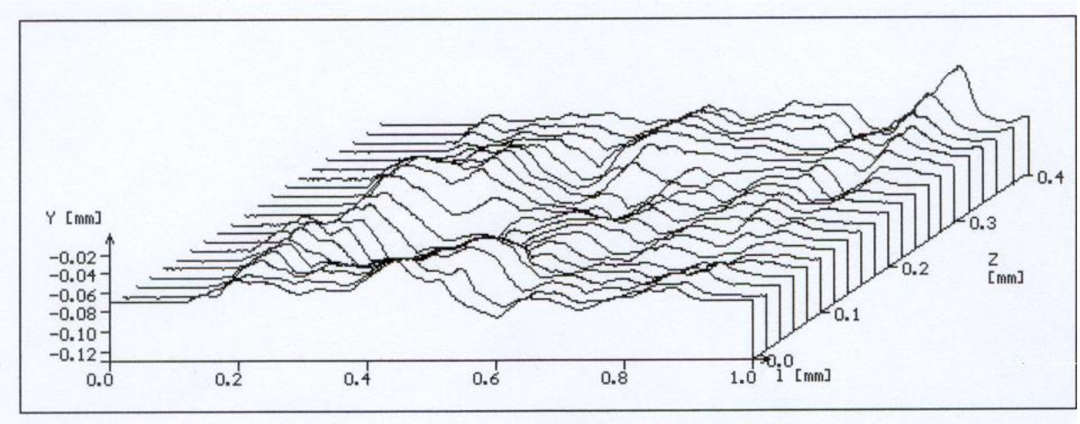

(a) P = 150 MPa

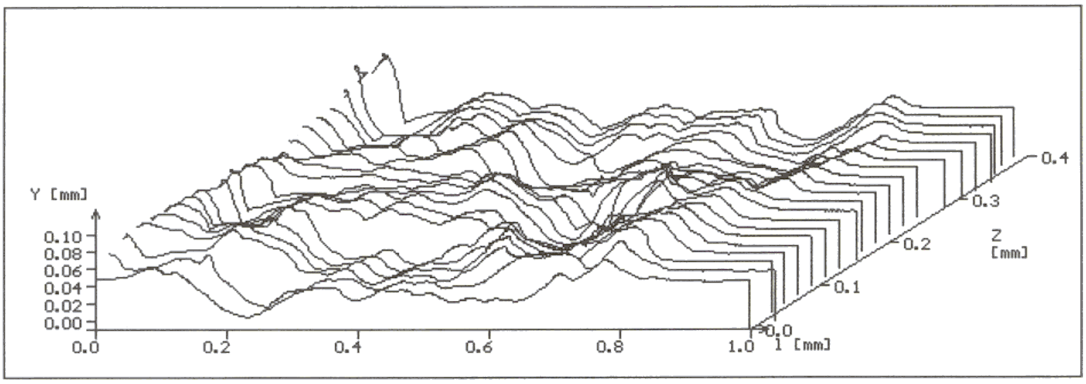

(b) P = 350 MPa

Fig. 1. 3D Topographies of AWJ machined surfaces for two different pressures

d_n=0.3 mm, d_m= 0.9 mm, S=3 mm, u=12 m/min, abrasive: garnet, Mesh No: 80, $\dot{m}_a$ =0.5g/s

As pressure increases, from 150 MPa to 350 MPa, the penetration depth of the abrasive particle increases and so does the raised material surrounding craters. When the abrasive particle ceases its interaction with the workpiece and leaves the surface, the workpiece material is piled up at the sides of the crater. This raised material is presumably removed by subsequent particles. It constitutes the basis for the striation marks that appear in the deformation wear zone. It is clearly shown from these AWJ topographies, that burr formation in the deformation wear zone exists from the early time when the abrasive particle impinges the workpiece material at normal incidence. ''Hashish pointed out the existence of burrs at the exit side of thin sheets near the side of the deformation wear zone. The reason was attributed to the bending force and the material in the deformation wear zone was assumed to be bent rather than removed.[7]''. It must be noted that, increasing flow rate tends to increase the density of abrasive particle impingements on the same area. This is shown in Fig. 2, whereas the increase in the number of craters is slight due to the low pressure used.

4.2 ***Workpiece stresses***

It has been widely thought that, impingement of the abrasive particle on the workpiece surface, causes extremely high stresses to build up, which lead to local plastic deformation at the site of impact. Consequently, for a short instance, intensive stresses that frequently produce a local site of damage develop in the workpiece material. In ductile materials, where the primary failure mechanism is plastic flow, the damage appears in the form of a conical crater around the impact site with the apex exactly in the center. Figure 3 shows the results of the flow stresses, calculated by FEM, acting at the cutting interface. At the beginning of impact, Fig. 3 (b), the

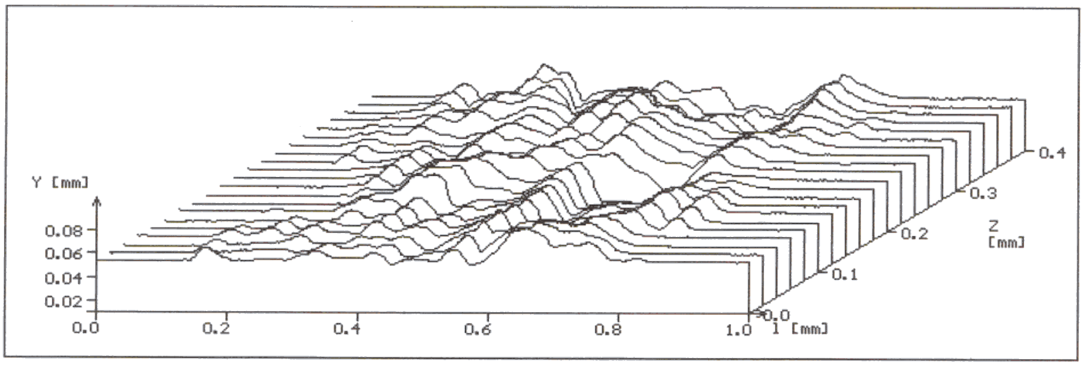

(a) $\dot{m}_a$ =0.1 g/s

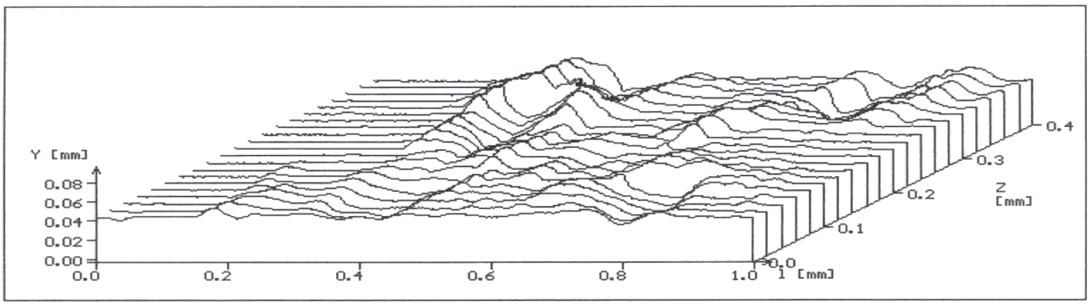

(b) $\dot{m}_a$ =0.25 g/s

Fig. 2. Effect of abrasive flow rate on AWJ surface topographies
P=100 MPa, d_n=0.3 mm, d_m= 0.9 mm, S=3 mm, u=12 m/min, abrasive: garnet, Mesh No: 80

abrasive particle completely exchanges its high momentum with the workpiece material. As a result, elastic compressive stresses, Fig. 3 (c), where the abrasive particle is removed for clarity, are developed at the impact site, the maximum of which is exactly at the center. It is seen from the figure that, elastic pressure waves penetrate into the workpiece material causing it to soften. As the abrasive particle penetrates into the workpiece material, the impact site is subject to considerable plastic flow stresses, which exceed the rupture strength of the workpiece material causing local plastic deformation, Fig. 3 (d). At this stage, plastic stress waves are developed under the location of the recently formed kerf. The propagation of this compression wave in the bulk of the workpiece material that surround the impact site, is clearly visible in the Figure. The magnitude of the calculated flow stresses is somewhat consistent with the value suggested by ‘‘Hashish to be E/14 for steel, where (E) is the modulus of elasticity.[9]’’. It is also clearly seen from the figure that, at this stage plastic deformation becomes very localized at the site of impact. At the final stage of abrasive-workpiece interaction, Fig. 3 (e), a permanent micro crater has been generated which is trying to get rid of its residual stresses to remain stable. This final stage usually takes more time than the impact moment duration itself.

The erosion behavior of the workpiece material under the action of AWJ impact could be explained, with the aid of Fig. 4, for deformation wear mode i.e. for large angles of impact. For high pressures, e.g. 270 MPa, very high compressive flow stresses significantly develop at the center of the impact site as a result of abrasive particle impact on the workpiece surface. These stresses build up from the moment of impact (A), until the point of maximum interaction; at (B). These stresses exceed the flow strength of the material under similar impact loading. As a result, flow stresses sharply develop in the workpiece material causing material to flow at very high strain rate. It results in the formation of AWJ kerf with the maximum stresses found to be concentrated in the center of that kerf. It must be noted that, as pressure increases, the depth of cut also increases. This is explained by the fact that flow stresses also increase with pressure. It is obviously seen that flow stresses significantly increase as pressure increases. Hence, The most effective means for producing deeper AWJ kerfs is to increase pressure. Extremely high values of stresses, that we got, may be attributed to the small size effect of the impacting abrasive particle. It impinges on a minute area on the workpiece surface, of the

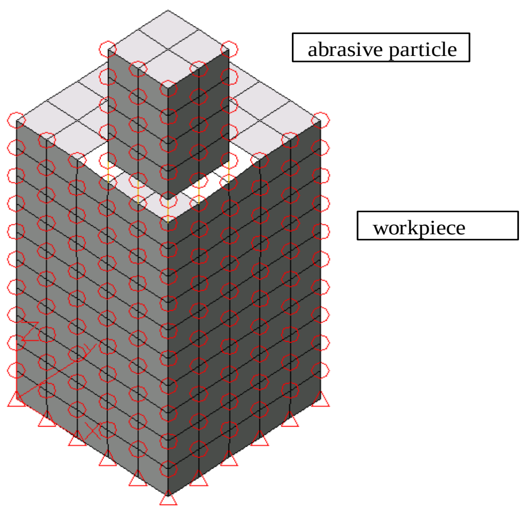

(a) Initial FE model

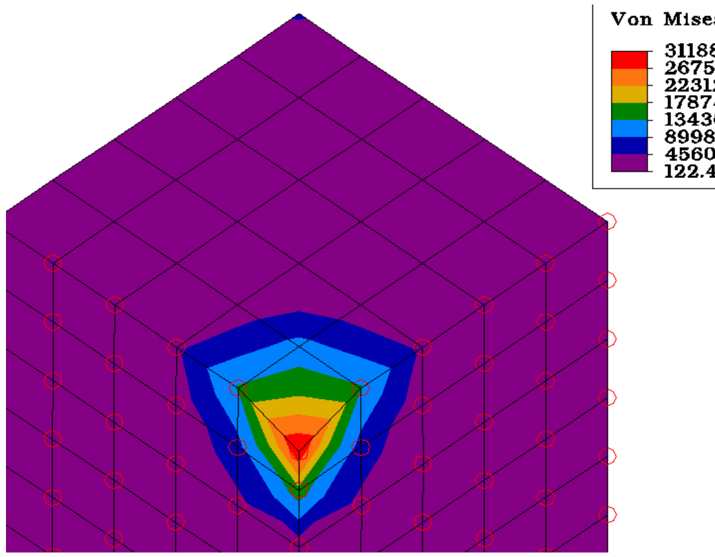

(d) t = 0.73 μs

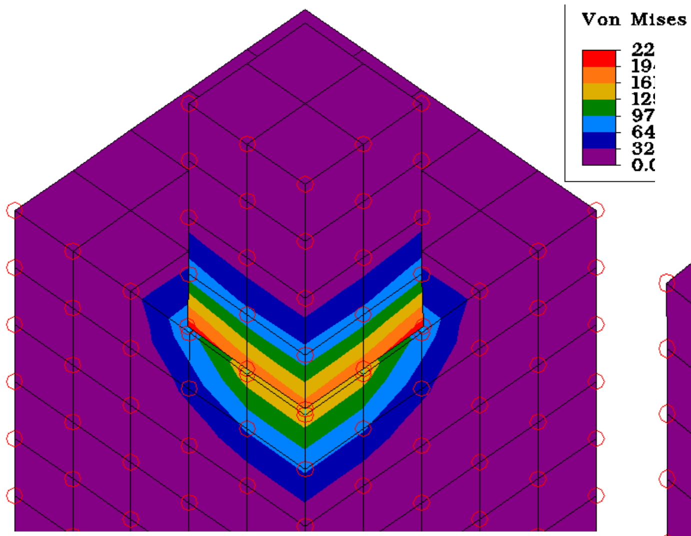

(b) t = 0.28 μs

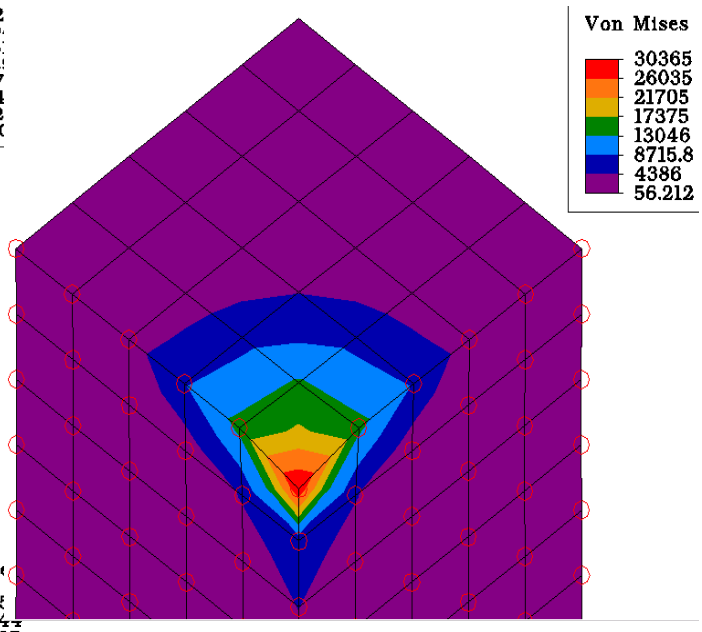

(e) t=1.3 μs

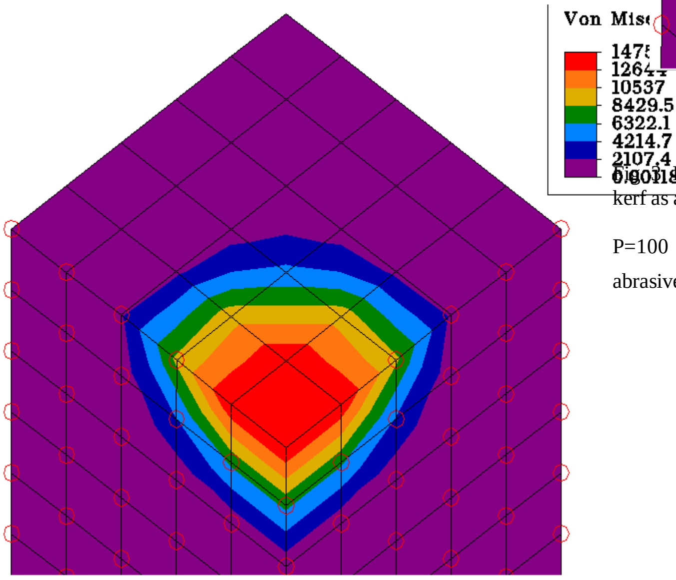

(c) t = 0.28 μs

Fig. 3 FE results of the development of Von Mises stresses in AWJ kerf as a result of impact

P=100 MPa, d_n=0.3 mm, d_m= 0.9 mm, S=0.1 mm, u=12 m/min, abrasive: garnet, Mesh No: 80, $\dot{m}_a$ =0.5 g/s size of a grain. This result is consistent with the results obtained by Hashish ‘‘who pointed out this fact and attributed it to the small size effect.[9]’’. Shortly after the abrasive particle starts to reflect from the workpiece material, flow stresses suddenly decrease significantly as seen in Fig. 4, from (B) to (C). This is due to a sudden increase in both maximum and minimum principal stresses. Afterwards, while the abrasive particle is retracting itself from the workpiece material, beyond point (B), the latter quickly starts to get rid of most of stresses it gained during the previous impact. Finally, this results in high residual compressive stresses, specially at the area adjacent to the center of the AWJ kerf. The repeated collisions of a large number of particles will form a plastically deformed surface layer. The resulting deformation hardening increases the strength. It has then become relatively hard and brittle and can no longer be plastically deformed. For lower pressures, i.e. below 90 MPa, the generated flow stresses are not capable of producing deep AWJ kerfs as they only leave a light impression on the workpiece surface. This leads to the conclusion that there is a critical pressure beyond which erosion starts effectively. Below this velocity, there is no possibility to cut materials with AWJ. This observation is also consistent with Hashish ‘‘who estimated this pressure to be 90 MPa for steel.[9]’’.

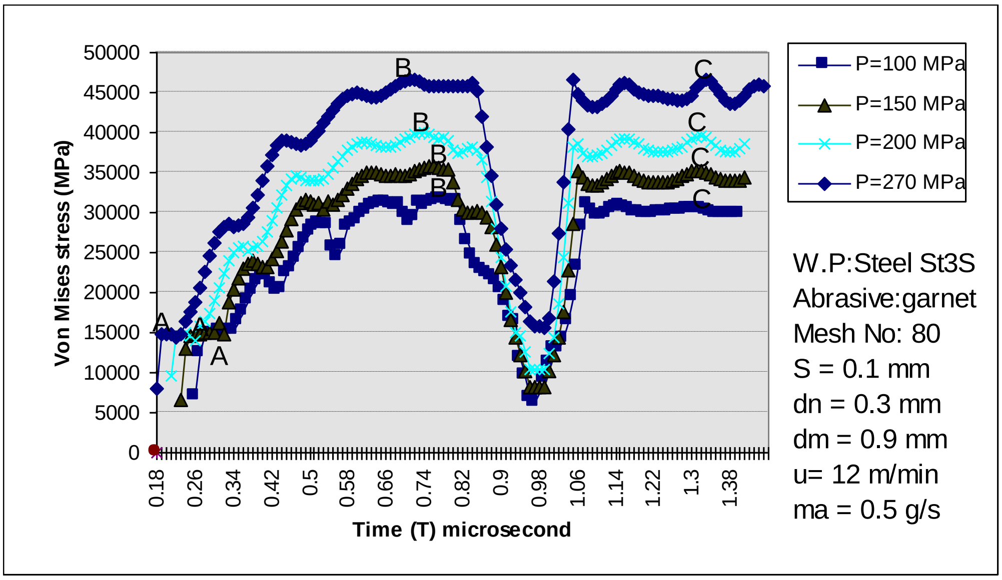

Fig. 4. Development of flow stresses with time for different pressures

4.3 *Scanning electron microscopy observations*

Figure 5 shows a general view taken for the small cavities, produced on an AWJ machined surface, as a result of individual abrasive particle impact. It’s clearly seen from the photomicrograph that, the workpiece surface is subject to plastic deformation rather than a wear process, since no workpiece material is removed in the form of chips. This is typical for normal impact on ductile workpiece materials.[9,10].

Fig. 5. SEM photograph of an AWJ machined surface showing craters as a result of individual abrasive particles impact
P=100 MPa, d_n=0.3 mm, d_m= 0.9 mm, S=3 mm, u=12 m/min, abrasive: garnet, Mesh No: 80, $\dot{m}_a$ =0.5 g/s

Plastic deformation is also clearly shown in Fig. 6 (a) and Fig. 7, where SEM photos are taken across and along the AWJ kerf respectively. The high speed impact causes material to flow out of the crater because of the high compressive stresses developed at the interaction region, between the abrasive particle and the workpiece material. It could also be seen that the maximum deformation occurs in the center of the impact site as accurately predicted using FEM. It can be seen from Fig. 6 (b), that the developed FE model accurately simulates the shape and the depth of the AWJ cavity. The deviation of the theoretical results from the experimental ones may be due to the error in calculating the abrasive particle velocity which is equal to 8% for the current conditions. Mixing tube nozzle wear, pressure fluctuations and inaccuracies in calculating abrasive flow rate could also contribute to this deviation. Also, the fracture of the abrasive particles during impingement with the workpiece surface and their nonuniformity reduces the actual depth of cut.

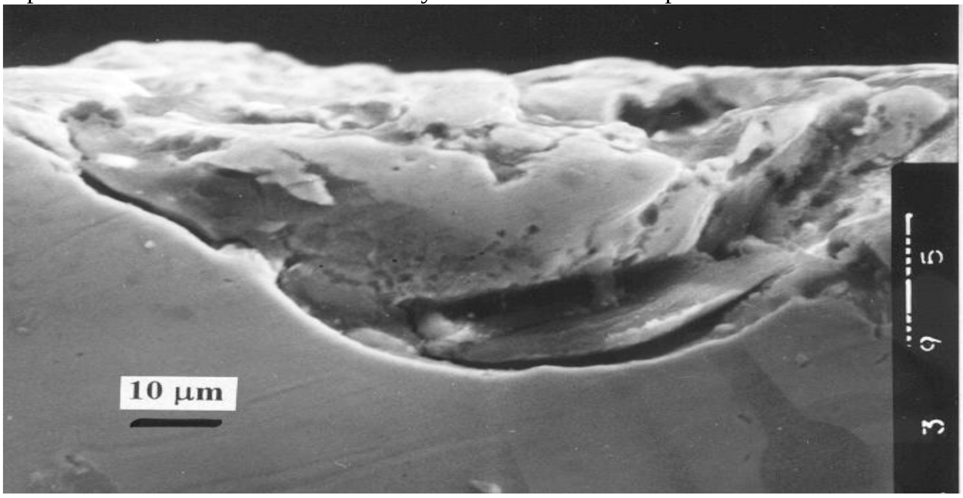

(a) SEM photograph taken across AWJ kerf showing a micro crater

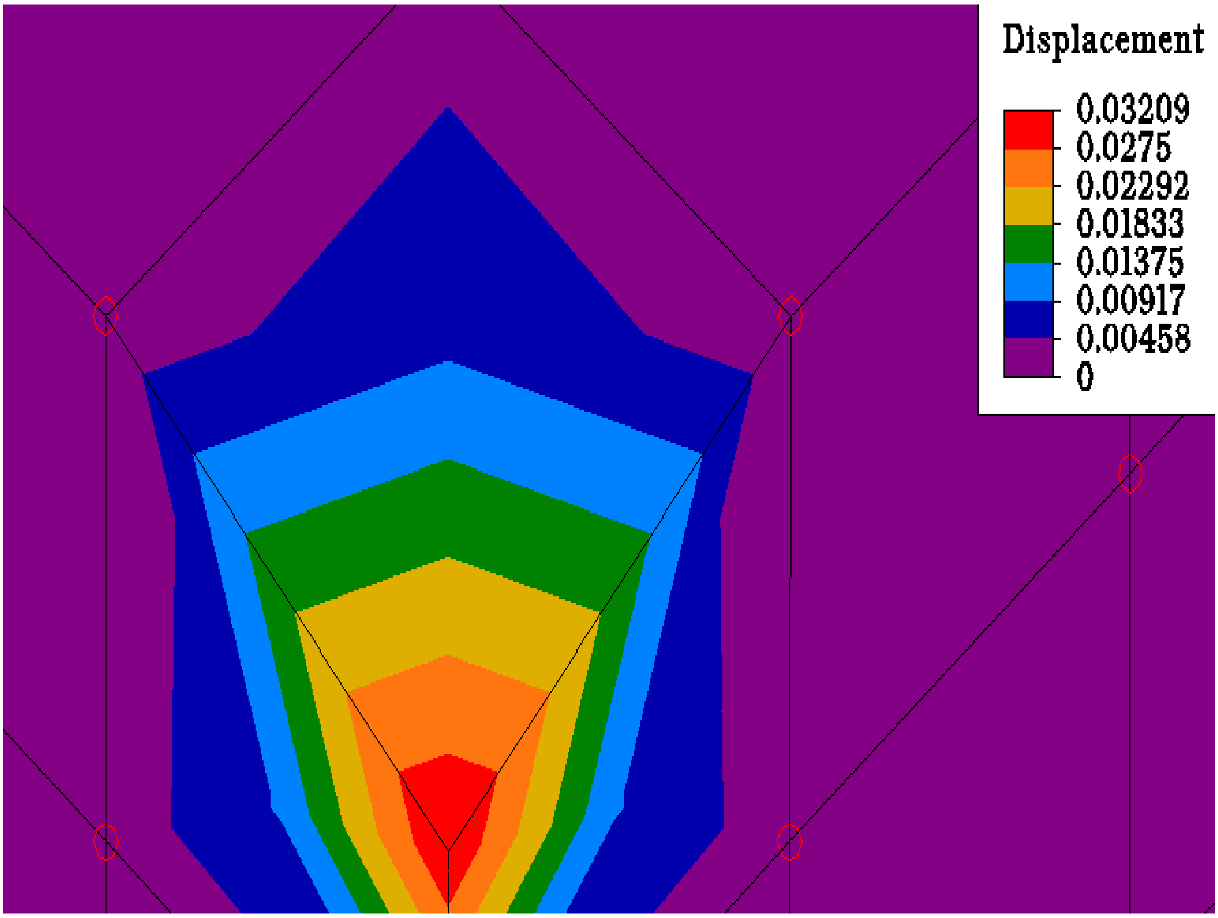

(b) The above micro crater obtained by FEM (t = 1.8 µs)

P=100 MPa, d_n=0.3 mm, d_m= 0.9 mm, S=3 mm, u=12 m/min, abrasive: garnet, Mesh No: 80, $\dot{m}_a$ =0.5 g/s

Fig. 6. Comparison between FE model and experimental results

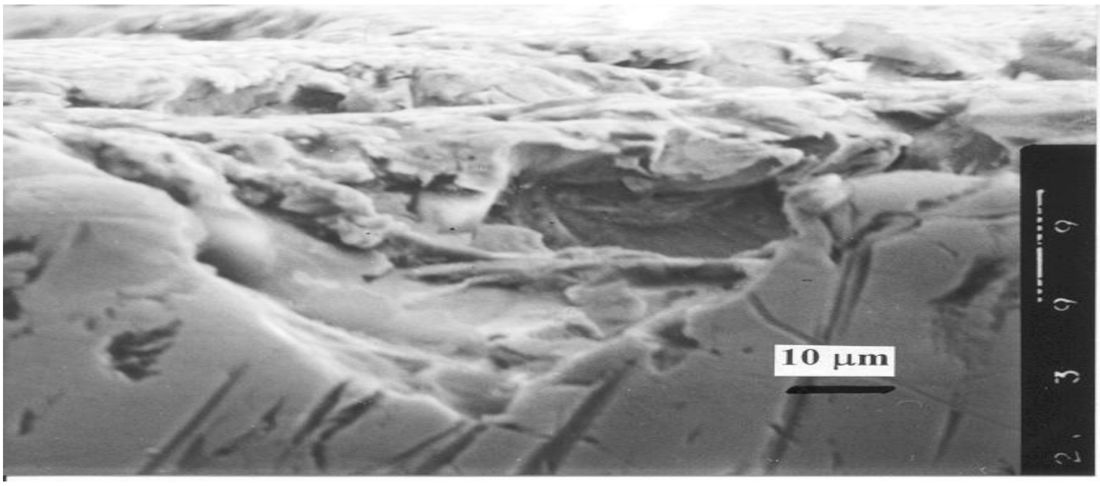

Fig. 7. An SEM photograph taken along AWJ kerf showing the severe plastic deformation as a result of abrasive particle impact
P=100 MPa, d_n=0.3 mm, d_m= 0.9 mm, S=3 mm, u=12 m/min, abrasive: garnet, Mesh No: 80, $\dot{m}_a$ =0.5 g/s

5 A Proposed Mechanism of Material Removal

An erosion mechanism could be proposed, with the aid of Fig. 3 and supported by SEM photographs shown in Fig. 6 and Fig. 7, as follows. At the moment of impact, the maximum elastic compressive stress is developed at the center of the impact site, surrounded by a ring of lower value stresses. As a result, elastic pressure waves are generated below the impact site that extend to a depth smaller than the length of the abrasive particle. Afterwards, the stress ring is decreased in diameter and the pressure waves are becoming more concentrated in the center. As stresses which are generated both on the surface of the workpiece material and below the impact site exceed the rupture strength of the workpiece material under such high strain rate erosion, circumferential plastic deformation is produced in a ring around the center of the impact site, extending to a depth of one half of the length of the abrasive particle. As a result, a micro AWJ kerf is generated and it is widened as the abrasive particle penetrates into the workpiece material. At this stage, plastic deformation becomes very localized at the center of the impact site. Afterwards, plastic pressure waves, are quickly spreading below this severely plastically deformed impact site. As a result of this softening effect, plastic deformation continues at the impact site.

ACKNOWLEDGMENTS

The authors would like to express their gratitude to the Polish Committee for Scientific Research (KBN), for its financial support of the present work under grant No. 7 T08E 021 16.

CONCLUSIONS

As a result of the current investigation of the mechanism of material removal in abrasive waterjet machining (AWJM) process, the following conclusions could be drawn:

1. Impingement of the abrasive particle on the workpiece surface, causes extremely high stresses to build up, which lead to local plastic deformation at the site of impact. The workpiece material plastically flows under the effect of the generated high speed pressure waves in two directions; downwards at the center of the impact site, and upwards, at the peripheral edges of the recently formed cavity. As a result, a central crater is developed at the center of the impact site.
2. Based on the results of both FE model and AWJ experiments, an erosion mechanism is proposed.

REFERENCES

1 W. Goldsmith, Bouncing from one collision to the next, Applied Mechanics Review, **52**, 8 (1999) R27-R43.

2 T. Babul, Selected phenomena of dynamically loaded materials, The Archive of Mechanical Engineering, **XLV**, 4 (1998) 325-339.

3 S. Ando, Y. Mine, K. Takashima, S. Itoh, H. Tonda, Explosive compaction of Nd-Fe-B powder, Journal of Materials Processing Technology, **85 (**1999) 142-147.

4 W. F. Alder, Waterdrop impact modeling, Wear, **186-187 (**1995) 341-351.

5 E. S. Geskin, W. L. Chen, S. S. Chen, F. Hu, M. E. H. Khan, S. Kim, Investigation of anatomy of an abrasive waterjet, in proc. 5th Amer. Waterjet Conf., 1989, 217-230.

6 N. S. Gue, H. Louis, G. Meier, J. Ohlsen, Abrasive waterjet cutting improvement of the surface quality, in proc. 4th Pac. RIM Int. Conf., Water Jet Technology, 1995, 469-480.

7 M. Hashish, Characteristics of surfaces machined with abrasive-waterjets, Transactions of the ASME, Journal of Engineering Materials and Technology, **113** (1991) 354-362.

8 A. I. Hassan and J. Kosmol, Finite element modeling of abrasive waterjet machining, in proc. 15th Int. Conf., Jetting Technology, 2000.

9 M. Hashish, A model for abrasive-waterjet (AWJ) machining, Transactions of the ASME, Journal of Engineering Materials and Technology, **111 (**1989) 154-162.

10 I. Finnie, Erosion of surfaces by solid particles, Wear, **3** (1960) 87-103.